SIGNIFICANCE OF DSMC COMPUTED AEROTHERMAL ENVIRONMENTS IN THE RAREFIED REGIME FOR ATMOSPHERIC ENTRY MATERIAL RESPONSE

Arnaud Borner, Science and Technology Corporation at NASA Ames Research Center (arnaud.p.borner@nasa.gov)
Jeremie B.E. Meurisse, Science and Technology Corporation at NASA Ames Research Center (jeremie.b.meurisse@nasa.gov)
Nagi N. Mansour, NASA Ames Research Center (nagi.n.mansour@nasa.gov)

Introduction

During Mars atmospheric entry, the Mars Science Laboratory (MSL) was protected by a 4.5 meters diameter ablative heatshield assembled in 113 tiles [1]. The heatshield was made of NASA's flagship ablative material, the Phenolic Impregnated Carbon Ablator (**PICA**) [2]. Prior work [3] compared the traditional **one-dimensional and three-dimensional** material response models at different locations in the heatshield. It was observed that the flow was basically one-dimensional in the **nose and flank regions**, but three-dimensional flow effects were observed in the outer flank.

SPARTA: https://sparta.sandia.gov
DPLR: https://software.nasa.gov/software/ARC-16021-1A
PATO: https://software.nasa.gov/software/ARC-16680-1

The objective of this work is to study the effects of the aerothermal environment on the material response. We extend prior work [3] by computing aerothermal environments using the direct simulation Monte Carlo (**DSMC**) code **SPARTA** [4] and the CFD code Data Parallel Line Relaxation (**DPLR**) [5]. SPARTA is used to compute environment in the **rarefied regime** prior to 48.4s of entry where the **Knudsen number** is such that the Navier-Stokes equations can be inaccurate. Similarly to previous work, the DPLR software is used to compute the hypersonic environment for laminar then turbulent boundary layer assumptions from **48.4 s up to 100 s** after Entry Interface (EI) along the MSL 08-TPS-02/01a trajectory.

We observe that extending the aerothermal environments to times prior to 48.4 s **modifies the thermal response of the heat shield at the surface and in-depth**; however **the effects on the recession are minimal**. Additionally, using the assumption of a turbulent boundary layer versus a laminar one leads to **higher surface and in-depth temperatures**, **larger recession**, and a **displacement of the peak heating and peak recession location**.

Aerothermal environments from SPARTA and DPLR

The MSL flight environment was simulated using the following assumptions for both the CFD and DSMC simulations:

- Super-catalytic wall BC: CO_2 and N_2 recombination to freestream mole fractions
- Radiative equilibrium wall with $\varepsilon = 0.89$
- Mars atmosphere $y_{CO2} \approx 0.97$ and $y_{N2} \approx 0.03$
- 8 species and 24 reactions(12 forward + 12 backward): Mitcheltree model [6]
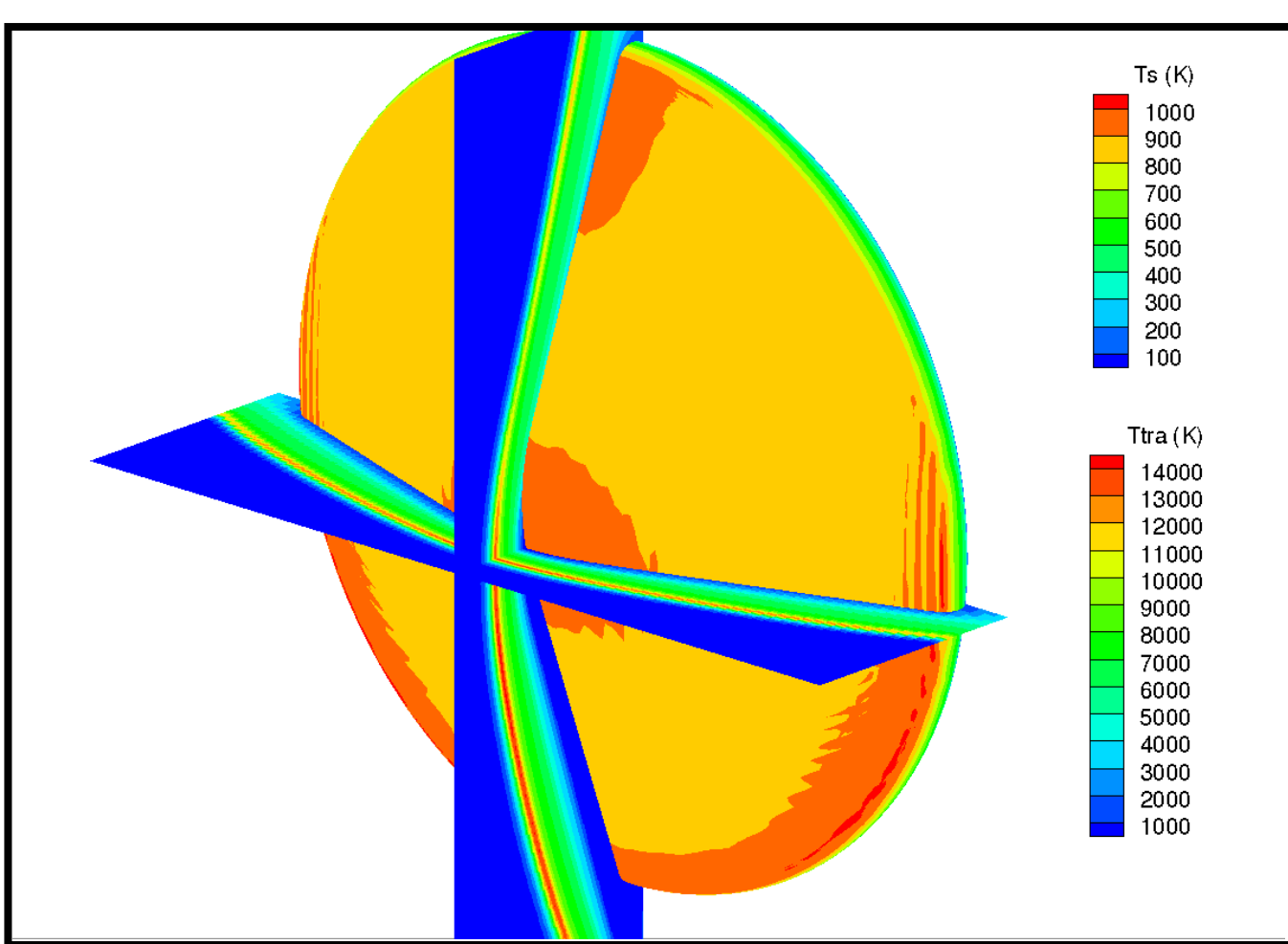- Park hypersonics correction to vibrational relaxation

Differences between CFD and DSMC:
- DPLR uses a 2 temperature model and SPARTA a 3 temperature model
- Laminar or turbulent (Menter SST 2-equation model) boundary layer model in DPLR
- Binary diffusion coefficients from Gupta collision integrals [7] in DPLR
- SPARTA uses Variable Soft Sphere (VSS) model with high temperature transport calibration
- Parker equation for rotational relaxation and Millikan-White equation + Park correction for vibrational relaxation in SPARTA

Fig. 1 Surface and translational temperature contours at 40 s of entry computed using DSMC

Fig. 2 MEDLI Integrated Sensor Plug (MISP) locations [3]

Fig. 3 Evolution in time of pressure (p_w) and BLE enthalpy (h_e) at the front surface (laminar and turbulent environments)

Fig. 4 Evolution in time of heat transfer coefficient (C_H)at the front surface (laminar and turbulent environments)

- Shock standoff distance decreases with decreasing altitude
- Strong non-equilibrium in shock at high altitudes
- Angle of attack varies from 30 deg at high altitude to 16 deg after 48 s of entry
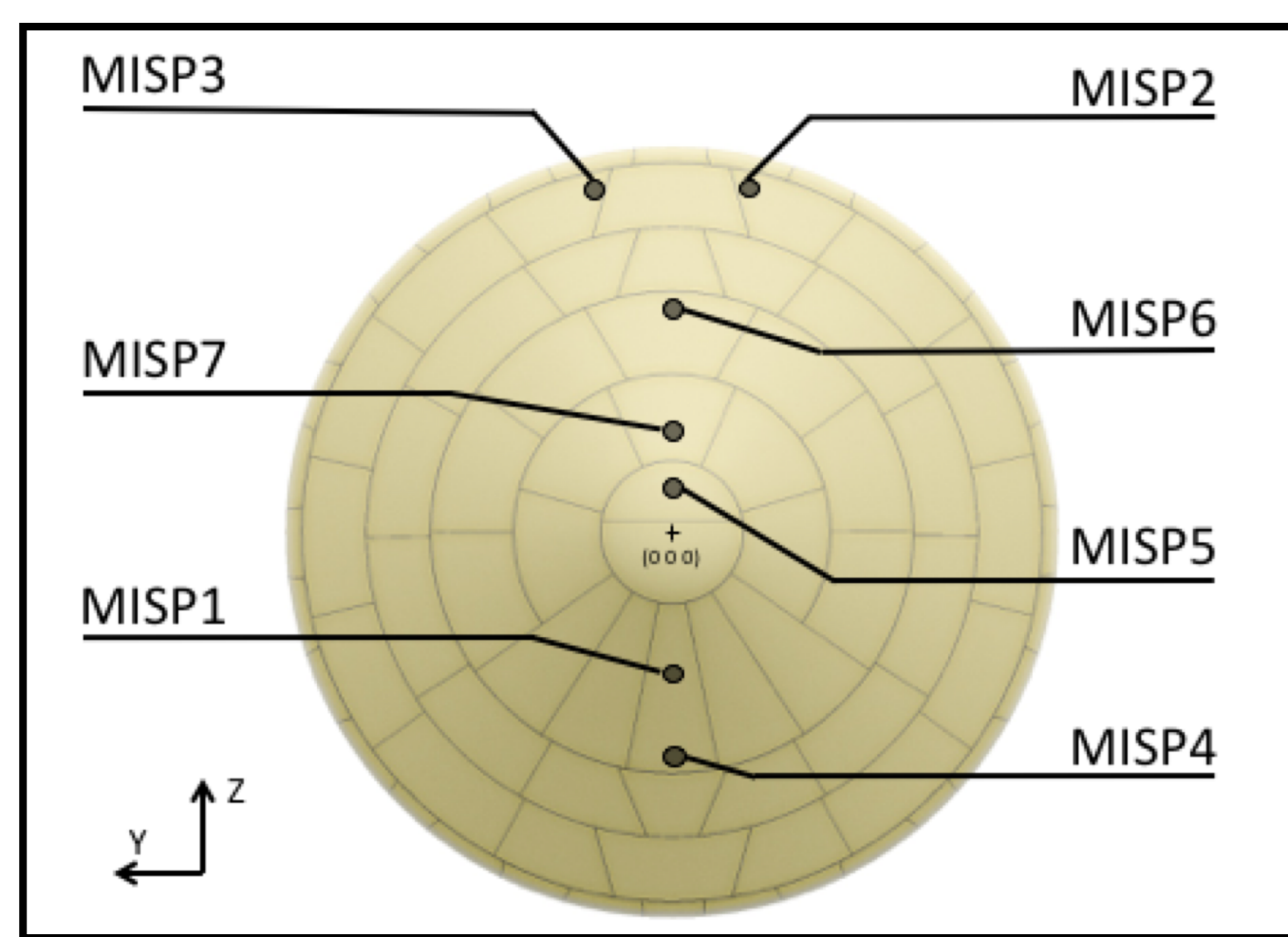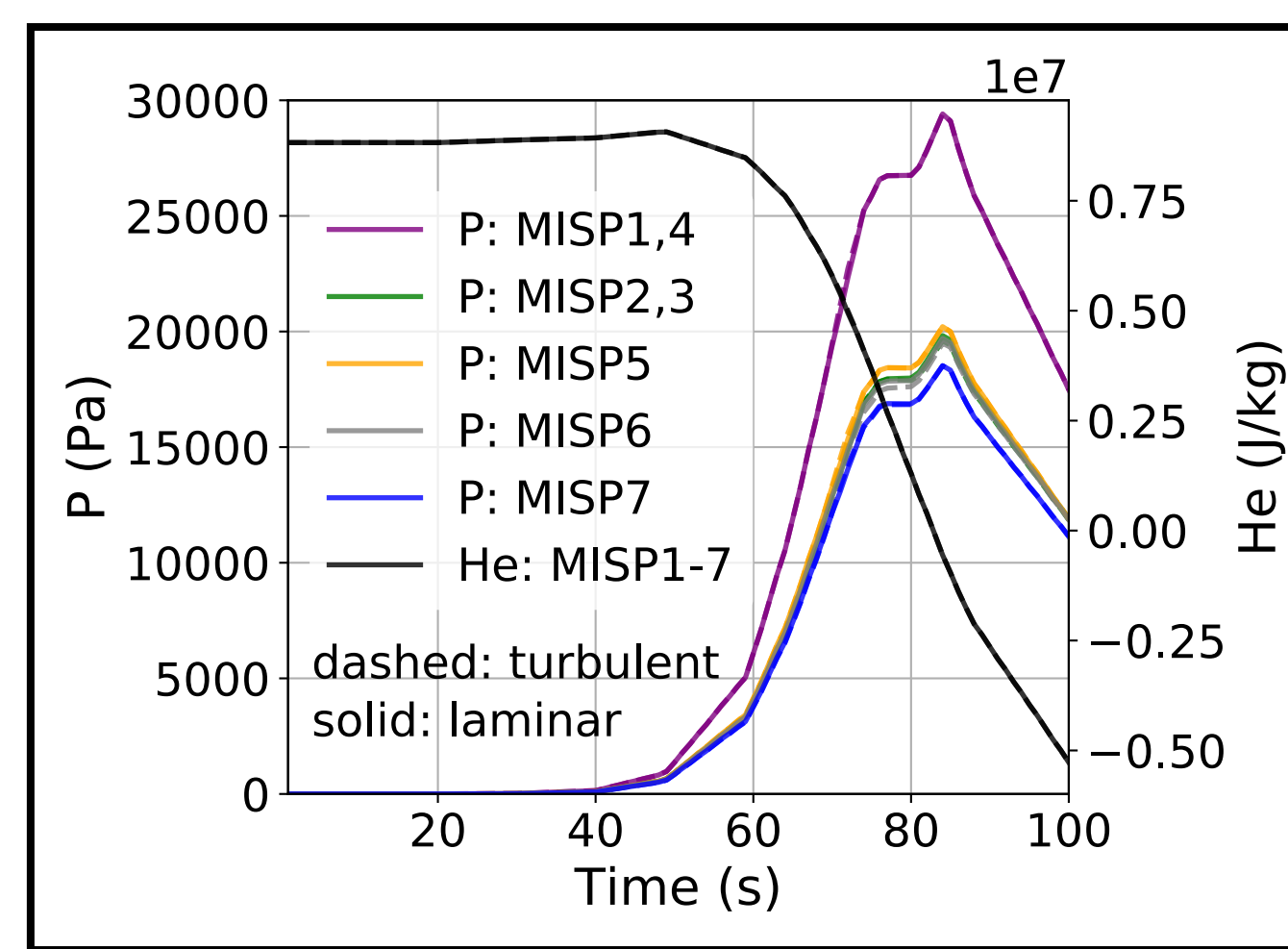
- 7 plugs with 4 thermocouples each
- Nominal depth: TC1: 2.54 mm, TC2: 5.08 mm, TC3: 11.43 mm, TC4: 17.78 mm [8]
- MISP4 located at the stagnation point
- Assembly of 113 PICA tiles
- TACOT material properties used in PATO

- Peak of pressure occurs around 84 s, highest at plugs 1 and 4, close to stagnation point
- BLE enthalpy is high until 60 s then drops to negative values after 84 s
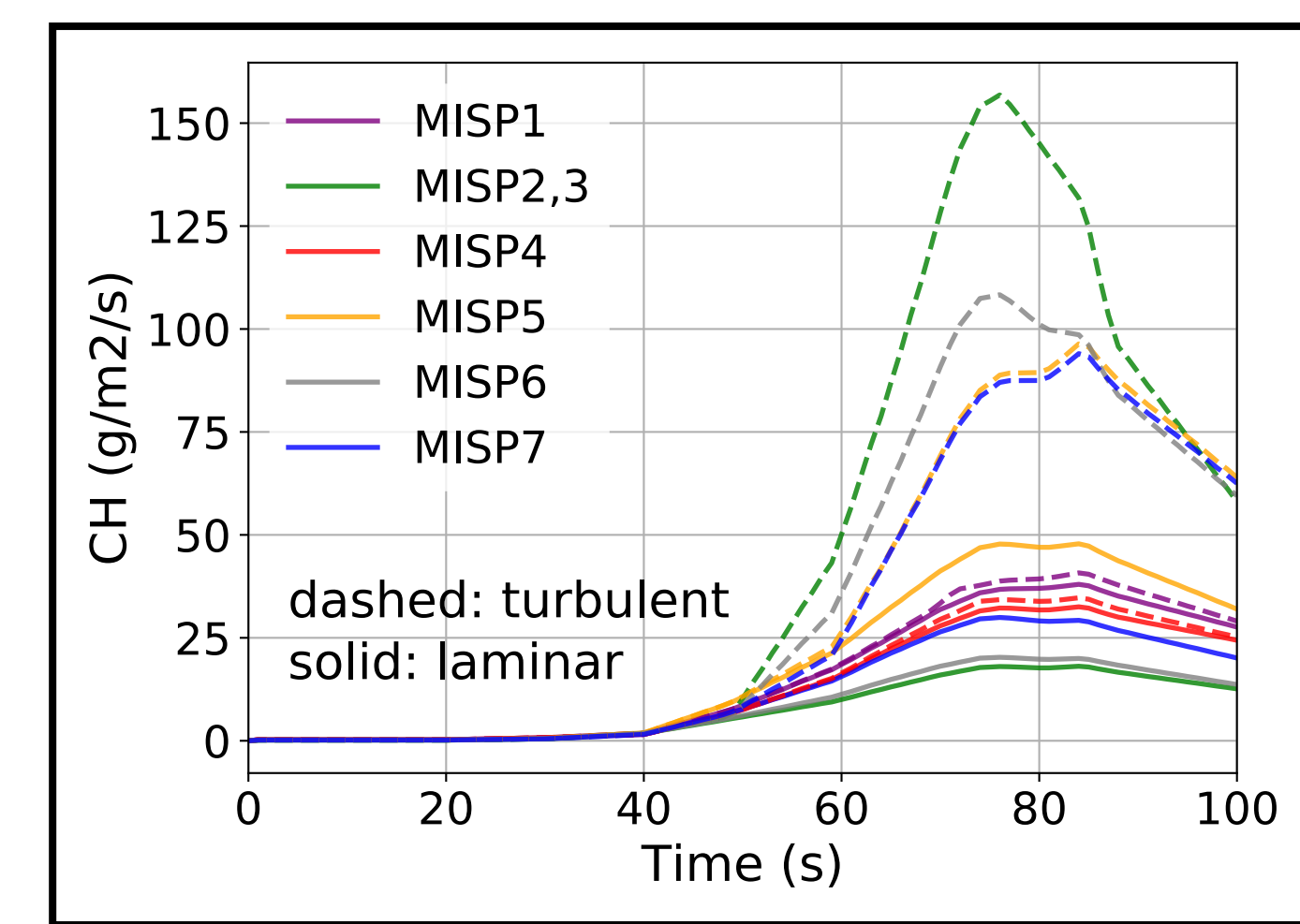- No difference between laminar and turbulent environments

- C_H computed from PATO Boundary Layer utility and BLAYER [9]
- Two peaks in heat transfer coefficient appear around 75 s and 85 s
- Maximum heating occurs at MISP5 for laminar and MISP2,3 for turbulent
- Heating much higher for turbulent

Material response from PATO

The Porous material Analysis Toolbox based on OpenFOAM (**PATO**) [10, 11] is used for the material response calculations. The governing equations are volume-averaged forms of solid mass, gas mass, gas momentum and total energy conservation, including pyrolysis gas production. The thermodynamics and chemistry properties are computed using the **Mutation++** library [12]. The boundary conditions at the heatshield front surface are interpolated in time and space from the aerothermal environment at discrete points of the MSL trajectory [3], using a Galerkin projection. For this study, the Theoretical Ablative Composite for Open Testing (**TACOT**) database developed by the TPS community was used to define the porous material properties. TACOT is a fictitious material that was inspired from low density carbon/phenolic ablators. The boundary layer edge (BLE) quantities from DPLR are extracted using a curvature-based method with the **BLAYER** code [9]. For the DSMC results, a Boundary Layer utility was created in PATO and an edge-based method is used (location of BLE such that $h_e = 99.5$ % of h_∞). The turbulent environment case strongly increases the surface temperature compared to laminar environment, and relocates the area of maximum temperature from the nose to the leeside flank region (Fig. 5). We compute the PATO material response of the MSL heatshield in a **monolithic 3D configuration**, with the Martian aerothermal environments derived from **DPLR only** and **DSMC+DPLR**. The laminar and turbulent solutions are in agreement until 50 s of EI, however, **the surface temperature reaches values up to twice higher** in the case of the **turbulent** environment (Fig. 6). For MISP4, in-depth thermal effects are as important as surface thermal effects especially before 60 s (Fig. 7). Fig. 8 shows the **surface recession** computed in PATO with the highest recession at MISP5 as expected for a **laminar aerothermal environment**, and at MISP2,3 for a **turbulent aerothermal environment**. The recession is 4 times larger for the turbulent environment. Almost no recession is observed before 60 s due to the low heat flux. Only subtle differences in the recession are found between DPLR only and DSMC+DPLR derived environments.
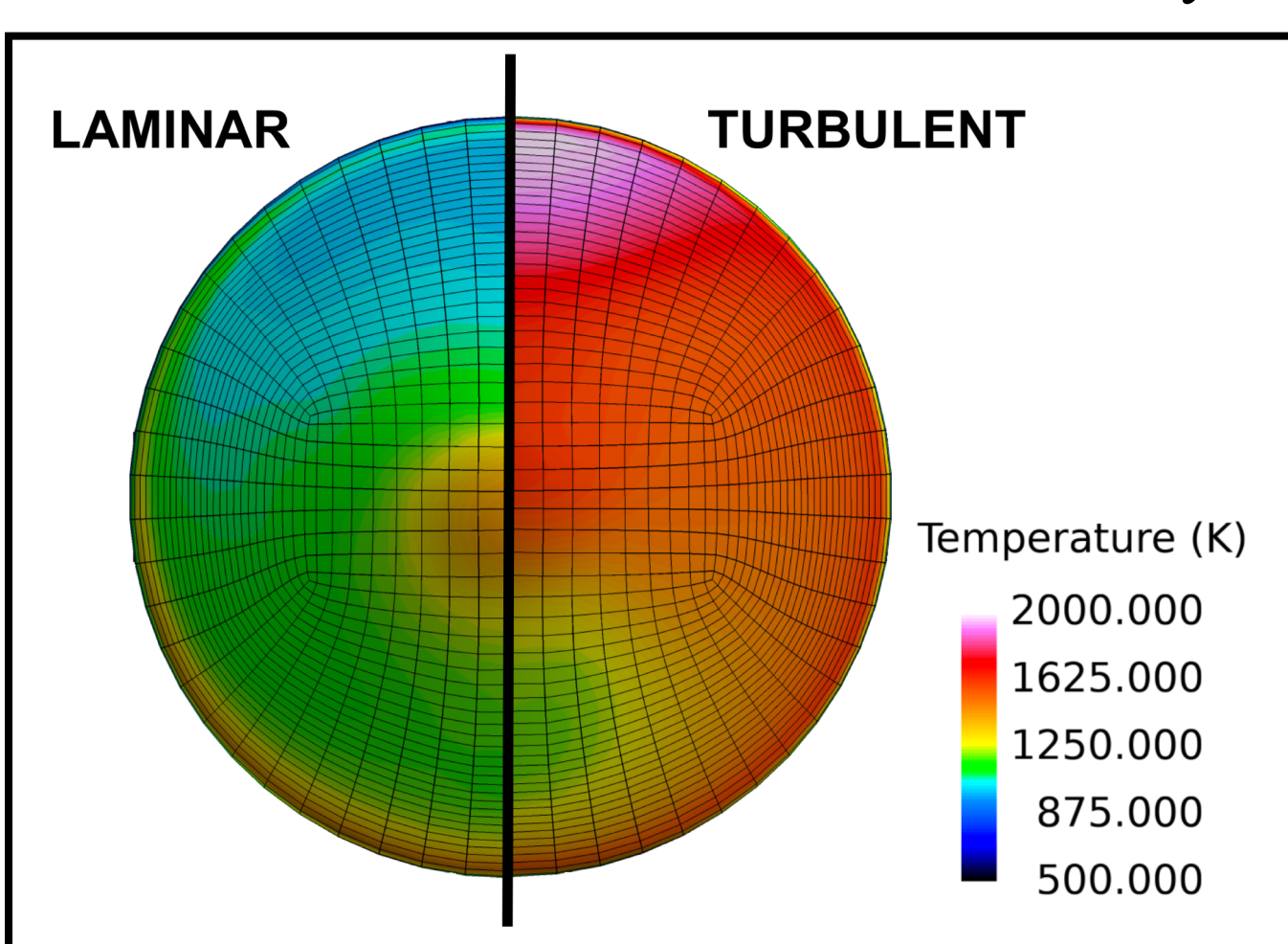

Fig. 5 3D-view of PATO output (temperature T_w) at heat shield front surface (78s of MSL entry) for laminar and turbulent environments
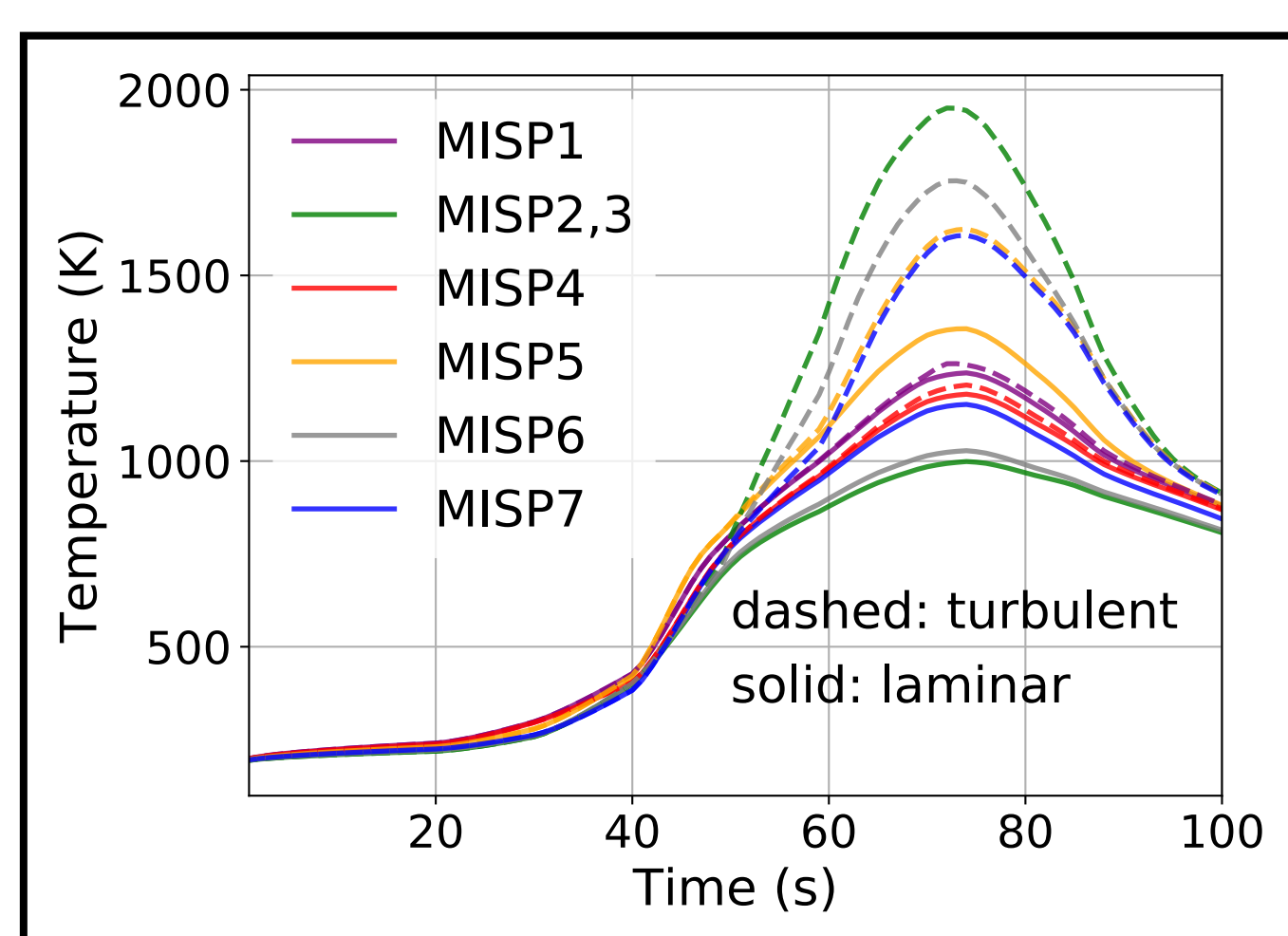

Fig. 6 PATO surface thermal response at the MISP locations (laminar and turbulent environments)
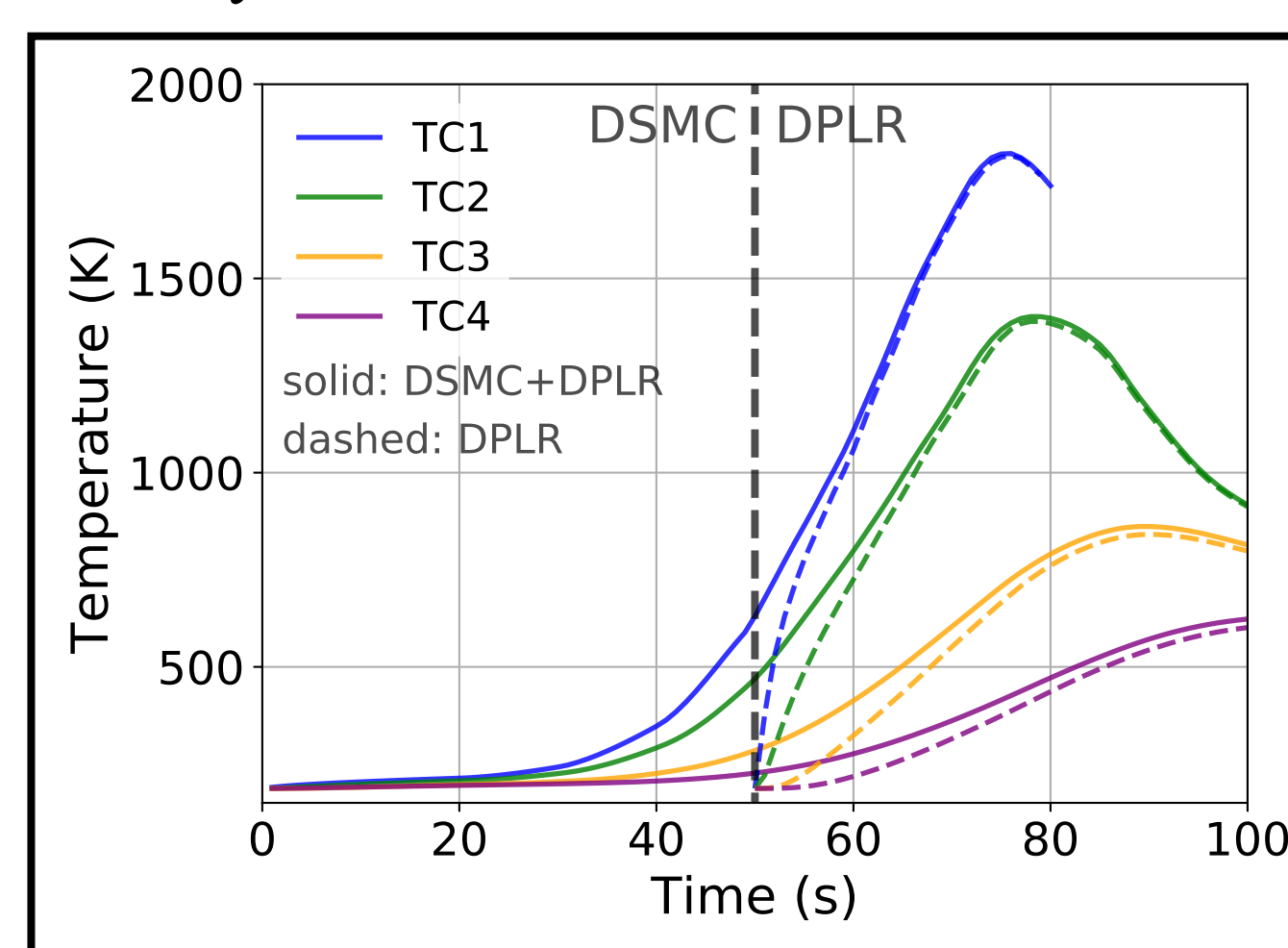

Fig. 7 PATO in-depth thermal response at MISP2 (turbulent environment)
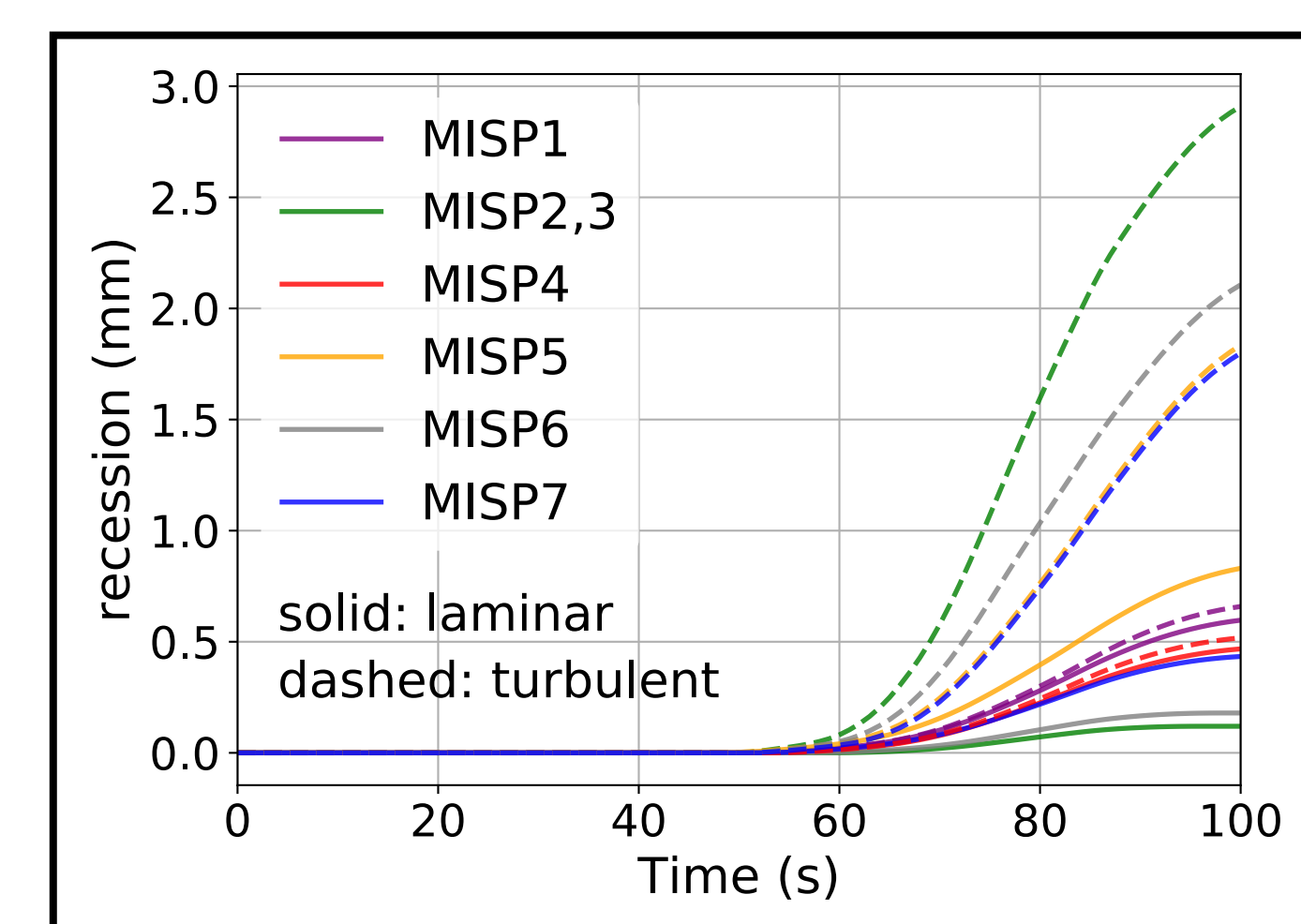

Fig. 8 PATO surface recession at the MISP locations (laminar and turbulent environments)

References

[1] K. T. Edquist, et al. (2009) *AIAA Paper* 2009-4075.
[2] M.J. Wright et al. (2009) *AIAA Paper* 2009-4231.
[3] J. B.E. Meurisse et al. (2018), *Aerosp Sci Technol*, 76, 497-511.
[4] M. A. Gallis et al. (2014), *AIP Conf Proc* 1628, 27.
[5] M. J. Wright et al. (2009), *DPLR Code User Manual: Acadia-Version 4.01.1.*
[6] R. Mitcheltree et al. (1995), *JSR* 32 (5), 771-776.
[7] R. Gupta et al. (1990), *NASA-RP*-1232.
[8] T. R. White et al. (2013), *AIAA Paper* 2013-2779.
[9] D. Saunders and D. Prabhu. (2018), *BLAYER User Guide*, NASA/TM-2018-219749.
[10] J. Lachaud and N. N. Mansour (2014), *J Thermophys Heat Tran*, 28, 191–202.
[11] J. Lachaud et al. (2017), *Int J Heat Mass Tran*, 108, 1406–1417.
[12] J. B. Scoggins and T. E. Magin (2014), *AIAA Paper* 2014-2966.